
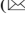







# Implementation and Use of the Bounding Surface Plasticity Geomaterial NTUASand02

Tony Fierro<sup>1</sup>  , Davide Noè Gorini<sup>2</sup> , Massimina Castiglia<sup>1</sup> ,  
and Filippo Santucci de Magistris<sup>1</sup> 

<sup>1</sup> University of Molise, Campobasso, Italy  
tony.fierro@unimol.it

<sup>2</sup> Sapienza University of Rome, Rome, Italy

**Abstract.** The numerical description of the undrained cyclic behaviour of sandy soils still represents a challenging issue in evaluating the response of geotechnical systems in seismic conditions. To this end, a large number of constitutive models have been developed over the years, with positive implications and limitations in capturing the soil response. In particular, the bounding surface plasticity theory has proven to be a valuable framework for reproducing the hardening soil response under both drained and undrained conditions. To increase the computational capabilities of the analysis framework OpenSees in assessing the dynamic response of soils, in the present study the well-known bounding surface plasticity model developed by Papadimitriou and Bouckovalas (2002) [1], referred to as NTUASand02, has been implemented as a new NDMaterial in OpenSees. The new source code can be used under both plane-strain and three-dimensional conditions. It provides an advanced analytical formulation that implies a delicate evaluation of a set of input parameters controlling the hardening features and pore water pressure build-up. Hence, a sensitivity analysis at the scale of the volume element is here proposed to point out clearly the influence of the constitutive parameters on the response. First, the effectiveness of an existing calibration procedure of the input parameters is shown with reference to a well-characterized sand. Then, monotonic and cyclic triaxial tests are simulated to address the influence of a variation in the model parameters requiring a trial-and-error calibration.

**Keywords:** Soil Constitutive Modelling · NTUASand02 · Liquefaction · Implementation · Parametric Analysis · OpenSees

Multiple evidence during past earthquakes witnessed severe damages generated by the soil liquefaction on structural systems, often causing the collapse of the whole system [2, 3]. Consequently, wide research activity has been developed over the years toward a shared understanding of the phenomenon and more reliable design procedures. To this aim, a number of constitutive models devoted to the description of the hysteretic behavior of saturated, coarse-grained soils was developed in recent years within different theoretical frameworks. Among them, the bounding surface plasticity theory turned out to be particularly efficient by virtue of the elegance of the formulation and the ability in simulating the evolution of the soil hardening response, as well as the liquefaction triggering under undrained conditions.

With reference to this framework, the present paper describes the implementation in OpenSees [4] together with the verification and validation procedure of the bounding surface constitutive model developed by Papadimitriou and Bouckovalas (2002) [1]. The effect of some critical model parameters on the monotonic and cyclic response is finally critically assessed.

## 1 The Papadimitriou and Bouckovalas (2002) Constitutive Model

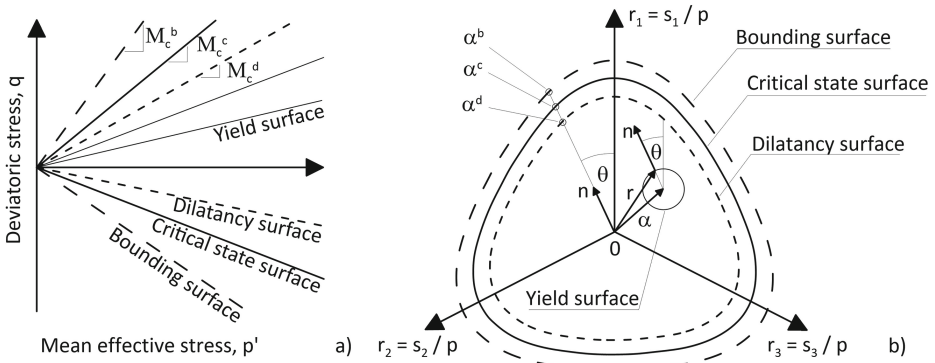
The Papadimitriou and Bouckovalas (2002) constitutive relationship [1], referred herein to as NTUASand02, is an evolution of the elastic-plastic bounding surface model proposed by Manzari and Dafalias (1997) [5], and represents the multi-axial generalization of the model developed by Papadimitriou et al. (2001) [6]. In the following, the main features of NTUASand02 are recalled.

A logarithmic variation of the void ratio at the critical state,  $e_{cs}$ , with the mean effective stress,  $p'$ , is assumed in NTUASand02 and the state parameter is defined as  $\psi = e - e_{cs}$  [7]. The hardening response develops when the stress state lies on the yield surface and the stress increment points outwards of the surface.

The elastic-plastic stress-strain relationship depends on the distance between the current stress state and three surfaces: dilatancy, critical state, and bounding, according to the mapping rule schematically shown in Fig. 1 and described in detail in [1]. Each surface is described by a cone with the apex in the origin of the  $p'$ - $q$  invariants plane (Fig. 1a); the intersection between these surfaces and the  $\pi$ -plane is reported in Fig. 1b, in which  $r_i$  is the deviatoric stress ratio of the  $i^{\text{th}}$  principal effective stress,  $s_i$ , to the mean effective stress. In the  $\pi$ -plane, the conical yield surface is represented by a circle whose diameter is related to a constant parameter  $m$ , while its position relative to the hydrostatic axis is dictated by the deviatoric back-stress ratio tensor  $\alpha$ . Except for the critical state surface, the other surfaces evolve in the stress space according to a kinematic hardening law aimed at describing the behaviour of sandy soils under cyclic conditions, implying the evolution of  $\alpha$  as plastic strains occur. The tensor  $\alpha$  represents the internal variable of the constitutive model and a non-associated flow rule is included in the formulation.

The size of the dilatancy, critical state, and bounding surfaces on the  $\pi$ -plane depends on the state parameter  $\psi$ , while their shape is controlled by the Lode angle  $\theta$  based on the mapping rule.

Two additional, attractive aspects of the model consist of the definition of a scalar parameter  $h_f$ , scaling the plastic modulus to consider the fabric tensor evolution, and the non-linear Ramberg-Osgood formulation used to model the small-strain soil response (elastic regime) in a more realistic manner compared to more conventional linear elastic relationships.



**Fig. 1.** (a) Representation of the model surfaces on the  $p'$ - $q$  plane and (b) on the  $\pi$ -plane (reproduced from Papadimitriou and Bouckovalas, 2002 [1]).

## 2 OpenSees Implementation

NTUASand02 was implemented in OpenSees as a new NDMaterial. The source code is composed of a header file, containing the methods declaration, and a main file where the constitutive response is fully developed, under both plane-strain and three-dimensional conditions.

The main file contains the methods that define the material current state and its non-linear incremental response. Additional methods to calculate the state parameter, the Lode angle and the elastic moduli were implemented in the existing library. The possibility to use different integration schemes was included in the source code. The explicit modified Euler scheme with automatic error control and drift correction [8] was set as default because it represents the good compromise between required computational time and integration accuracy.

The material requires the definition of the parameters describing the elastic response ( $m, B, \nu, a_1, \gamma_1$ ), those referred to the critical state ( $e_{cs,a}, \lambda, M_c^c, M_c^c$ ), and those related to the effect of  $\psi$  on the peak strength ( $k_c^b$ ) and on the dilatancy surface ( $k_c^d$ ). Furthermore, additional input constants are the dilatancy ( $A_o$ ), the plastic modulus ( $h_o$ ), and the fabric ( $H_o, \zeta$ ) parameters; finally, the initial void ratio and the mass density need to be defined.

The constitutive model can be assigned to quadrilateral and hexahedral elements, including or not the hydro-mechanical coupling, under static or dynamic conditions. In a Tcl script, NTUASand02 is called through the command line in Fig. 2.

```
nDMaterial NTUASand02 $matTag $nu $VoidRatio $Mc $lambda_c $secs_a \\  
$P_atm $m $h0 $A0 $B $a1 $gamma1 $Me $k_bc $k_dc $H0 $zeta $SoilDen \\  
<$kappa $integrationScheme>
```

**Fig. 2.** Command line necessary for the use of NTUASand02 in OpenSees

Note that the parameters between `<...>` are optional, and the `IntegrationScheme` allows for the choice among the implemented integration schemes that are, currently: Forward Euler, Modified Euler with automatic error control, and 4<sup>th</sup> order Runge-Kutta that can be used by assigning to the variable the integers 5, 1, and 4, respectively. Either the Ramberg-Osgood para-elastic or the full elastic-plastic response can be adopted using the `updateMaterialStage` command. In particular, by assigning the integer 0, the user can exploit the para-elastic formulation, while the elastic-plastic formulation can be activated by switching `updateMaterialStage` to 1.

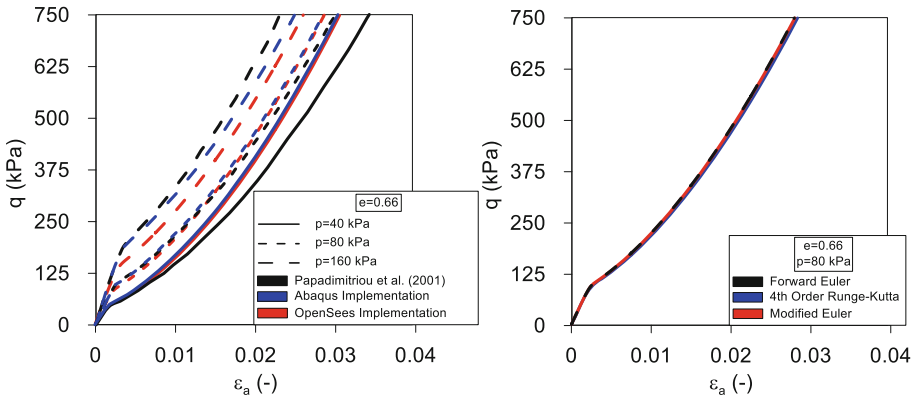
The element response is provided in terms of stress-strain relationship.

### 3 Code Validation and Use

The new source code was validated by simulating the monotonic and cyclic, drained and undrained, direct simple shear and triaxial tests carried out in the VELACS project [9] on Nevada sand. These simulations were also compared with previous numerical studies carried out in different analysis frameworks. The adopted constitutive parameters are those proposed in [1] for Nevada sand. In the following, only a small number of comparisons is discussed for brevity, while the reader can refer to Fierro (2022) [10] for further details.

#### 3.1 Validation of the New `NDMaterial`

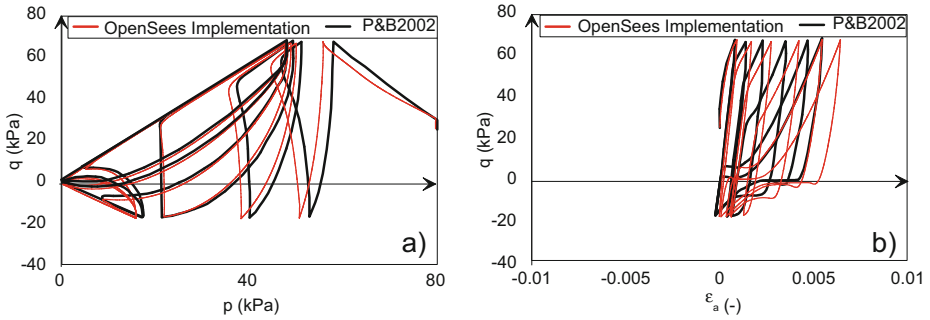
In this section, the simulations of undrained monotonic triaxial tests conducted on a Nevada sand sample with an initial void ratio equal to 0.66 are shown. Different values of effective confining pressure, i.e.,  $p' = 40, 80, 160$  kPa, were considered. The hexahedral element with hydro-mechanical coupling and single integration point, `SSPbrickUP` [11] was used. The deviatoric stress-axial strain response is shown in Fig. 3a and is compared to the response obtained by Papadimitriou et al. (2001) [6] in the original implementation of the model, and by Miriano (2010) [12] in Abaqus. Furthermore, the test having a confining pressure  $p' = 80$  kPa has been exploited to evaluate the performance of the three integration schemes: the default substepping Modified Euler with automatic error control, Forward Euler, and 4<sup>th</sup> order Runge-Kutta (Fig. 3b).



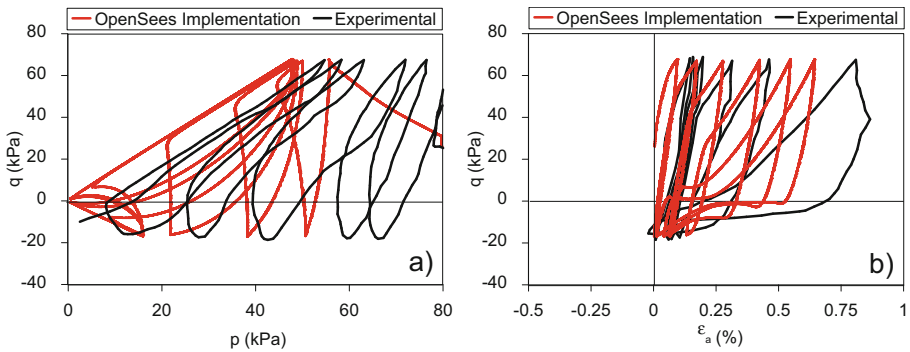
**Fig. 3.** (a) Comparison between the simulations of undrained monotonic triaxial tests obtained by Papadimitriou et al. (2001 [6], black curve), Miriano (2010 [12], blue curve), and adopting the OpenSees implementation (red curve); (b) comparison on the use of the different integration schemes available in the implemented, OpenSees source code.

The undrained monotonic tests highlight a good agreement between the results of the OpenSees implementation and those obtained by Miriano (2010) [12] in Abaqus. Some differences are observed by comparing the stress paths obtained by both OpenSees and Abaqus implementations compared to the original one by Papadimitriou et al. (2001) [6], probably due to some discrepancies in the implementation procedure of the material or in the solving algorithm of the system of equations. Furthermore, as observed in Fig. 3b, all the implemented integration schemes provide the same result.

Then, a cyclic triaxial test on a Nevada sand sample with a 0.66 initial void ratio ( $D_r = 40\%$ ) was reproduced by using a hexahedral finite element with hydromechanical coupling and four integration points (brickUP). The loading process consists of an anisotropic consolidation ( $p' = 80$  kPa,  $q = 26$  kPa) followed by a cyclic deviatoric stress with amplitude of 43.1 kPa. The resulting stress paths and hysteresis loops obtained in OpenSees are compared in Fig. 4 with the simulations carried out by Papadimitriou and Bouckovalas (2002) [1], while in Fig. 5 they are depicted together with the reference experimental data.



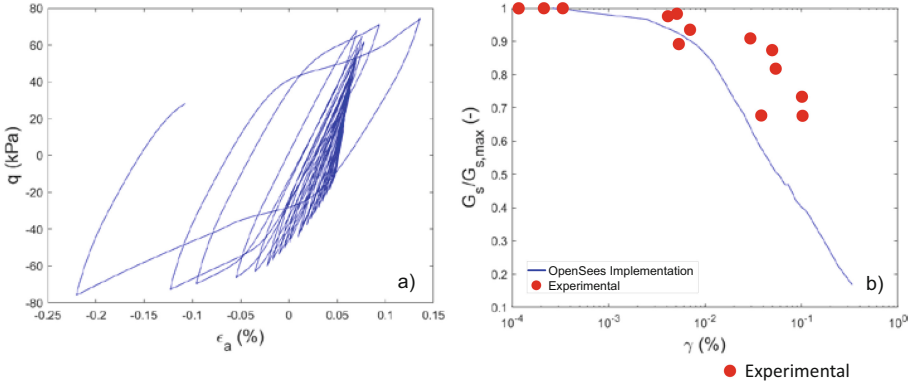
**Fig. 4.** (a) Stress paths in the  $p$ '- $q$  plane and (b) hysteresis loops obtained by Papadimitriou and Bouckovalas (2002 [1]; black curves), and OpenSees implementation (red curves).



**Fig. 5.** (a) Stress paths in the  $p$ '- $q$  plane and (b) hysteresis loops obtained from experimental data (Arulmoli et al. 1992 [9]; black curves), and OpenSees implementation (red curves).

As per the former comparison, the two implementations lead to very close results in terms of stress paths and hysteresis loops. However, the comparison between the simulations carried out in OpenSees and the experimental data highlights that the response at low-strain levels is not adequately reproduced by adopting the parameters calibrated in [1].

In order to investigate the evolution of the shear modulus  $G_s$  with the shear strain  $\gamma$  obtained through the considered calibration, a cyclic triaxial test on a Nevada sand volume element was simulated, considering a large number of loading cycles with an increasing amplitude. The resulting hysteresis loops and the associated normalized modulus reduction curve are shown in Figs. 6a,b, respectively. In the latter, the numerical result is compared with the experimental data provided by Arulmoli et al. (1992) [9] for Nevada sand. It highlights that the normalized modulus reduction is well simulated at small strain levels. For larger amplitudes, the shear modulus is visibly underestimated, pointing out the need of a more accurate calibration procedure of the model under cyclic loading.



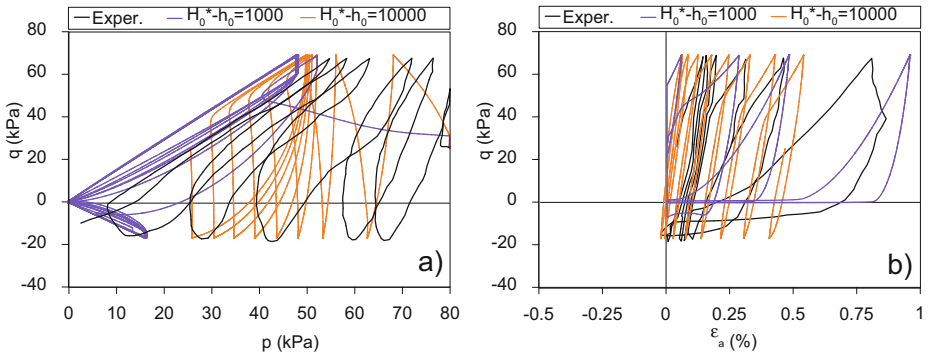
**Fig. 6.** (a) Comparison between the normalized modulus reduction curve obtained in OpenSees (blue curve) and the experimental data (Arulmoli et al., 1992 [9]; red dots); (b) simulated deviatoric stress-axial strain response.

## 4 Parametric Analysis

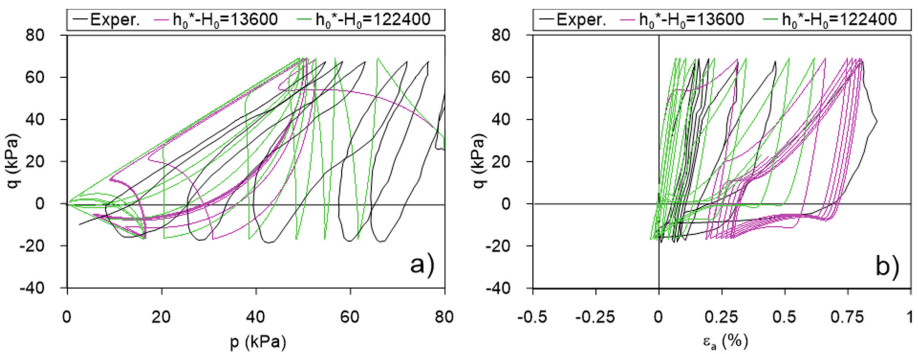
The simulations presented in Sect. 3 showed some limitations of the calibration proposed in [1] in reproducing the cyclic response of Nevada sand. The observed differences between experimental and numerical results can be due to both the adopted parameters and the constitutive formulation itself. As a common feature of advanced constitutive models for soil, they usually require a non-straightforward calibration of many parameters, employing trial-and-error procedures that inhibit the physical meaning of the parameters and their eventual correlation.

In the case of NTUASand02, the critical input parameters appear to be  $h_0$  and  $H_0$ , which affect the hardening response and need to be obtained by trial-and-error procedure. We investigated the effect of their variation using the new code implemented in OpenSees. The former constant ( $h_o$ ) is included in the definition of the parameter  $h_b$ , which accounts for the distance between the current stress state and its image stress point on the bounding surface, while  $H_o$  scales both the major principal stress and the state parameter at consolidation in order to consider directly their effect on the fabric tensor evolution and, consequently, on the plastic modulus. Papadimitriou and Bouckovalas (2002) [1] proposed a range of variation for  $h_0$  between 1000–10000, while acceptable values for  $H_0$  are bounded by the values 50000 and 100000. Considering these ranges, the effect of the extreme values of those parameters on the soil response is considered for  $h_o$ , while a wider range for  $H_0$  was analysed, from 13600 to 122400. The anisotropically consolidated cyclic triaxial test (confining pressure  $p' = 80$  kPa) on Nevada sand discussed in Sect. 3.1 was taken as a reference to analyse the variability of the parameters: the extreme value of a parameter was assigned to the material, keeping the other fixed to the reference value. As a result, four parameters permutations were analysed. In Figs. 7 and 8, the results of the simulations are shown in terms of stress paths and hysteresis loops, and the simulated curves are compared to

the experimental data. The asterisk (\*) indicates the reference value of a parameter, that is the one proposed by Papadimitriou and Bouckovalas (2002) [1] in the original calibration.



**Fig. 7.** (a) Stress paths in the  $p'$ - $q$  plane and (b) hysteresis loops obtained from experimental data (Arulmoli et al. 1992 [9]; black curves) and OpenSees implementation by changing the constitutive parameter  $h_0$  (violet and orange curves).



**Fig. 8.** (a) Stress paths in the  $p'$ - $q$  plane and (b) hysteresis loops obtained from experimental data (Arulmoli et al. 1992 [9]; black curves) and OpenSees implementation by changing the constitutive parameter  $H_0$  (magenta and green curves).

The stress paths and the hysteresis loops are qualitatively well reproduced even considering the upper and lower limit values of the parameters  $h_0$  and  $H_0$ ; however, the differences with the experimental data appears still remarkable. In particular, the reduction of  $h_0$  to 1000 (the parameter scaling the distance to the bounding surface) produces hysteresis loops and stress paths with an accelerated excess pore water pressure build-up (Figs. 7a, b), implying a faster liquefaction triggering. On the other hand, by assuming the upper limit  $h_0 = 10000$ , a stiffer response is obtained. With reference to  $H_0$  (it accounts for the effects of initial conditions on fabric evolution), it appears that by assuming  $H_0 = 13600$ , i.e., a value closer to the lower limit proposed in



[1], a more compliant response is reproduced if compared to the experimental data, while when its value approaches the upper limit, the response is closer to the experimental data (Figs. 8a, b), though still presenting some discrepancies. These results seem to indicate that there is no a unique combination of  $h_o$  and  $H_o$  providing good fitting and a reliable correlation between  $h_o$  and  $H_o$  is currently under investigation.

## 5 Conclusion

The current paper presented the implementation in OpenSees and validation of the constitutive model developed by Papadimitriou and Bouckovalas (2002) [1], referred to as NTUASand02. It was shown that the new source code can be successfully employed to simulate the response of coarse-grained soils under both monotonic and cyclic loading conditions in OpenSees.

The model was used to simulate different monotonic and cyclic triaxial tests, highlighting a good agreement with respect to the predictions obtained by different numerical platforms. However, the comparison with the experimental data highlights that the original parameters calibration [1] for Nevada sand is sometimes far from the observed behaviour under cyclic loading.

For this reason, the effect of the variation of the constitutive parameters  $h_o$  and  $H_o$ , requiring trial-and-error procedures was analysed, showing the significant sensitivity of the cyclic response to these parameters and pointing out the need for more systematic control of their identification.

## References

1. Papadimitriou, A.G., Bouckovalas, G.D.: Plasticity model for sand under small and large cyclic strains: a multiaxial formulation. *Soil Dyn. Earthq. Eng.* **22**, 191–204 (2002)
2. Ishihara, K., Yoga, K.: Case studies of liquefaction in the 1964 Niigata Earthquake. *Soils Found.* **21**(3), 35–52 (1981). [https://doi.org/10.3208/sandf1972.21.3\\_35](https://doi.org/10.3208/sandf1972.21.3_35)
3. Orense, R.P., Towhata, I., Chouw, N.: *Soil Liquefaction During Recent Large-Scale Earthquakes*. CRC Press, ISBN 9780429227158 (2014)
4. McKenna, F., Scott, M.H., Fenves, G.L.: OpenSees: nonlinear finite-element analysis software architecture using object composition. *J. Comput. Civil Eng.* **24**(1), 95–107 (2010)
5. Manzari, M.T., Dafalias, Y.F.: A critical state two-surface plasticity model for sand. *Geotechnique* **47**(2), 255–272 (1997)
6. Papadimitriou, A.G., Bouckovalas, G.D., Dafalias, Y.F.: Plasticity model for sand under small and large cyclic strains. *J. Geotechn. Geoenviron. Eng. ASCE* **127**(11), 973–983 (2001)
7. Been, K., Jefferies, M.G.: A state parameter for sands. *Geotechnique*, London **35**(2), 99–112 (1985)
8. Sloan, S.W., Abbo, A.J., Sheng, D.: Refined explicit integration of elastoplastic models with automatic error control. *Eng. Comput.* **18**, 121–154 (2001)
9. Arulmoli, K., Muraleetharan, K.K., Hossain, M.M., Fruth, L.S.: VELACS verification of liquefaction analyses by centrifuge studies Laboratory Testing Program Soil Data Report, Research Report, The Ea. Tech. Corp (1992)

10. Fierro, T.: Implementation and use of advanced constitutive models in numerical codes for the evaluation of the soil response under seismic loadings. Ph.D. Thesis, University of Molise (2022)
11. McGann, C.R., Arduino, P., Mackenzie-Helnwein, P.: A stabilized single-point finite element formulation for three-dimensional dynamic analysis of saturated soils. *Comput. Geotech.* **66**, 126–141 (2015)
12. Miriano, C.: Numerical modelling of the seismic response of flexible retaining structures. Ph. D. Thesis, Sapienza University of Rome (2010)